Sensorless field oriented control for five-phase induction motors with third harmonic injection and fault insensitive feature

F. WILCZYŃSKI*, P. STRANKOWSKI, J. GUZIŃSKI, M. MORAWIEC, and A. LEWICKI

Gdansk University of Technology, Faculty of Electrical and Control Engineering

Abstract. The paper presents a solution for sensorless field oriented control (FOC) system for five-phase induction motors with improved rotor flux pattern. In order to obtain the advantages of a third harmonic injection with a quasi-trapezoidal flux shape, two vector models, $\alpha_1-\beta_1$ and $\alpha_3-\beta_3$, were transformed into d_1-q_1, d_3-q_3 rotating frames, which correlate to the 1st and 3rd harmonic plane respectively. A linearization approach of the dual machine model in $d-q$ coordinate frames is proposed by introducing a new additional variable "x" which is proportional to the electromagnetic torque. By applying the static feedback control law, a dual mathematical model of the five-phase induction motor was linearized to synthesize a control system in which the electromagnetic torque and the rotor flux can be independently controlled. The results shows the air gap flux shape in steady as well transient states under various load conditions. Moreover, the implemented control structure acquires fault tolerant properties and leads to possible emergency running with limited operation capabilities. The fault-tolerant capability of the analyzed machine was guaranteed by a special implemented control system with a dedicated speed observer, which is insensitive to open-phase fault situation. The experimental tests have been performed with single and double-open stator phase fault. A torque measurement was implemented to present the mechanical characteristics under healthy and faulty conditions of the drive system.

Key words: fault tolerant control, field oriented control, five-phase induction machine, speed observer, third harmonic flux injection.

1. Introduction

In the last decades, the squirrel cage induction motor proved to be a simple and durable construction with low production costs. However, the industry is continuously searching for new technological solutions to satisfy the customer needs of enhanced economic performance and higher system reliability. Consequently an increasing number of publications are dedicated to the development of multiphase drives. One of the first publication, that presented the concept of a five-phase induction motor control appeared in 1969 [1]. From then on, many control strategies for three-phase applications, were implemented for multiphase drive systems including: open loop scalar control (U/f = const.) [2], FOC [1, 3–7], direct torque control (DTC) [4, 8, 9] as well as nonlinear control (multiscalar control) [10]. Nowadays, the development of the microprocessor and power electronics leads to manageable control possibilities for five-phase induction motors. A greater reliability, due to a higher number of phases provide the nominal load torque even with one faulted phase [11], lower torque pulsations [12] and a better cost-of-material ratio and the possibility of torque enhancement through the third harmonic injection [6, 10, 13–15]. A significant benefit of five-phase motor is the possibility of operation in case

of stator coil fault. The postfault performance of the five-phase machine has been analyzed in [16, 17], where one phase was opened. All the mentioned benefits make the five-phase machine a likely replacement of the three-phase induction motor. Nevertheless, the control of a five-phase induction motor proves to be a complex task [18]. This paper presents the implementation of an open phase fault insensitive non-linear FOC in sensorless configuration with third harmonic injection. A speed observer in dual structure was used [19, 20] to allow an independent control of the 1st and 3rd harmonic. The addition of the 3rd harmonic, that is three times faster than the 1st, leads to a quasi-trapezoidal flux, as shown in Fig. 1. The one phase open fault is tested in the proposed non-
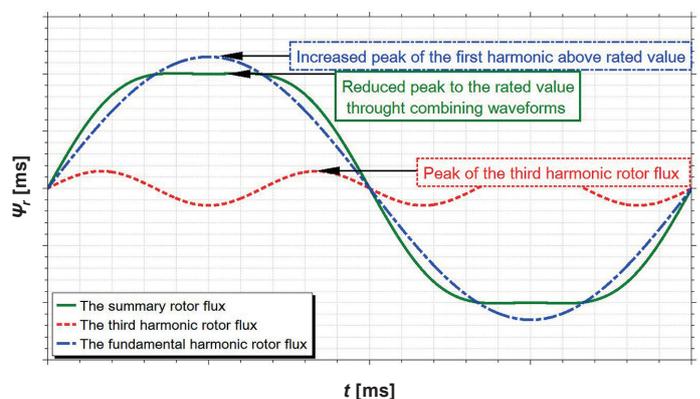

Fig. 1. Combined quasi-trapezoidal flux distribution waveform

*e-mail: filip.wilczynski@pg.edu.pl

linear FOC sensorless control and the new aspect referring to double-phase fault is also examined. The theoretical analysis is validated with experimental results for 5.5 kW five-phase induction motor drive (see Table 1).

Table 1
Data of five-phase squirrel-cage induction motor

Parameter	Value	Unit
Power – P_N	5.5	kW
Current – I_N	8.8	A
Phase voltage – U_N	173	V
Rotation speed – n_n	1423	rpm

2. System structure

2.1. Machine model in dual vector plane d_1-q_1, d_3-q_3. The machine model and the control structure were performed in two orthogonal, rotating planes to maintain a quasi-trapezoidal air gap flux distribution. The natural reference frame quantities can be transformed to the stator voltage, current and a rotor flux vectors, which are oriented in two uninfluenced vector planes d_1-q_1, d_3-q_3 (see Fig. 2).
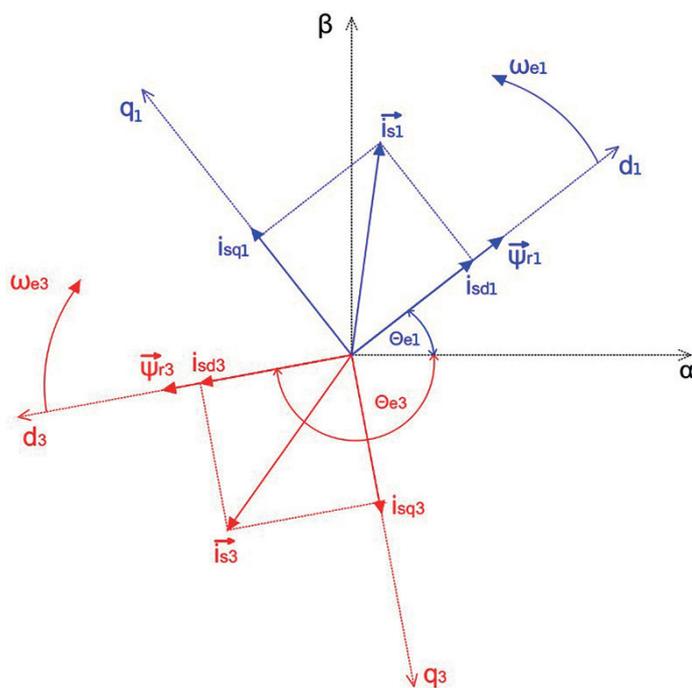

Fig. 2. Two rotating reference frames: d_1-q_1, d_3-q_3

The modified Fortescue transformation [19–22] for a multiphase structure was utilized to map the five-phase variables onto the two stationary orthogonal planes $\alpha_1-\beta_1$ and $\alpha_3-\beta_3$. After the calculation of the rotating angles Θ_{e1}, Θ_{e3} for the

d_1-q_1 and d_3-q_3 axes, the variables from $\alpha_1-\beta_1$, $\alpha_3-\beta_3$ to d_1-q_1, d_3-q_3 can be transformed to planes. Each of the planes is referred to the 1st and 3rd harmonic respectively. By setting a new additional variable $x_{(i)}$ proportional to the electromagnetic torque of the machine $\left(x_{(i)} = \Psi_{rd(i)} i_{sq(i)}\right)$ and on the basis of the static feedback control law, the mathematical model of the five-phase induction machine expressed in per unit system (see Table 2) in dual plane is described as follows:

Table 2
Definition of per unit values

Definition	Description
$U_b = \sqrt{5 U_N}$ B	Base voltage
$I_b = \sqrt{5} I_N$	Base current
$Z_b = U_b / I_b$	Base impedance
$T_b = (U_b I_b p)/\omega_0$	Base torque
$\Psi_b = U_b / \omega_0$	Base flux
$\omega_b = \omega_0 / p$	Base mechanical speed
$L_b = \Psi_b / I_b$	Base inductance
$J_b = T_b / (\omega_b \omega_0)$	Base inertia

$$\frac{dx_{(i)}}{d\tau} = \left(\frac{R_{s(i)} L_{r(i)}^2 + R_{r(i)} L_{m(i)}^2}{L_{r(i)}^2 L_{s(i)}^2 - L_{m(i)}^2 L_{r(i)}^2} + \frac{R_{r(i)}}{L_{r(i)}} \right) \left(-x_{(i)} + m_{1(i)} \right), \quad (1)$$

$$\frac{d\psi_{rd(i)}}{d\tau} = \frac{R_{r(i)}}{L_{r(i)}} \psi_{rd(i)} + R_{r(i)} \frac{L_{m(i)}}{L_{r(i)}} i_{sd(i)}, \quad (2)$$

$$\frac{di_{sd(i)}}{d\tau} = \left(\frac{R_{s(i)} L_{r(i)}^2 + R_{r(i)} L_{m(i)}^2}{L_{r(i)}^2 L_{s(i)}^2 - L_{m(i)}^2 L_{r(i)}^2} \right) \left(-i_{sd(i)} + m_{2(i)} \right), \quad (3)$$

$$\frac{d\omega_{r1}}{d\tau} = \frac{1}{J} \left(\frac{L_{m1}}{L_{r1}} x_1 - \frac{L_{m3}}{L_{r3}} x_3 - T_L \right), \quad (4)$$

where: $i_{s\alpha}$, $i_{s\beta}$, i_{sd}, i_{sq} – stator current vector components, $\psi_{r\alpha}$, $\psi_{r\beta}$, ψ_{rd}, ψ_{rq} – rotor flux vector components, $u_{s\alpha}$, $u_{s\beta}$, u_{sd}, u_{sq} – stator voltage vector components, ω_r – rotor angular speed, R_r, R_s – rotor and stator resistances, L_m – mutual-flux inductance, L_r, L_s – rotor and stator inductances, T_L – load torque, J – moment of inertia, τ – relative time. The new introduced control variables are described as $m_{1(i)}$ and $m_{2(i)}$. The subscript (i) signifies the corresponding vector planes. It can be seen from (1–4) that the proposed linearization of the five-phase induction machine model provides linear differential equations for torque and rotor flux in the i-th plane. The decoupling application can be used to decouple torque and rotor flux control. A change of the d_1-q_1 components will not influence the d_3-q_3 variables. From a control perspective, the two machine models in the i-th

www.czasopisma.pan.pl PAN www.journals.pan.pl

Sensorless field oriented control for five-phase induction motors with third harmonic injection and fault insensitive feature

plane act as two mechanically coupled and independent motors with shared magnetic structure (4).

2.2. Flux synchronization control.

The main aim of the 3rd harmonic injection is the optimization of air-gap flux distribution. To achieve the quasi-trapezoidal rotor flux distribution, the 1st and 3rd harmonic fluxes have to be adjusted (see Fig. 1) because the rotor flux vectors $\boldsymbol{\Psi}_{r(i)}$ in the *i*-th plane have the same relative rotating speeds. Therefore, the equation for the rotating flux speed in the both planes is as follows:

$$\omega_{e(i)} = \frac{R_{r(i)} L_{m(i)}}{L_{r(i)}} \frac{x_{(i)}}{\psi_{rd(i)}^2} + \omega_{r(i)}. \tag{5}$$

The five-phase induction machine with concentrated windings is associated with a non-zero value of mutual inductance [18]. By expressing the phase inductance through the Fourier series in connection with the stator-related angle and by taking into account the first two terms, the mutual inductance in the 2nd plane has a non-zero value [4]. This correlates with the three times higher pole pair number and the three times faster rotor angular speed in the 2nd plane in comparison to the 1st plane. The dependency between the rotor angular speed in the 1st and the 2nd plane is then:

$$\omega_{r3} = -3\omega_{r1}. \tag{6}$$

The reference value of electromagnetic torque x_3 providing the same flux relative rotating speeds can be deducted from (5) and (6) is as follows:

$$x_3^* = -3x_1^* \frac{R_{r1} L_{m1}}{L_{r1}} \frac{L_{r3}}{R_{r3} L_{m3}} \frac{\psi_{rd3}^2}{\psi_{rd1}^2}. \tag{7}$$

The equality of the rotor flux vectors $\boldsymbol{\Psi}_{r1}$, $\boldsymbol{\Psi}_{r3}$ relative rotating speeds does not ensure a quasi-trapezoidal distribution of the air gap flux. The proposed synchronization unit includes a rotor flux angle proportional controller whose output was added to the reference value of the electromagnetic torque in the 2nd plane (7) in order to align and lock the relative position between two rotor flux vectors $\boldsymbol{\Psi}_{r1}$, $\boldsymbol{\Psi}_{r3}$. It is important to convert the rotor flux vector angle position from the 1st to the 2nd plane in order to compare the Θ_{e1}, Θ_{e3} angles (see Fig. 3).

2.3. Observer of induction rotor speed.

The closed regulation system requires the induction machine state variables associated with a rotor flux and stator current. This paper presents an extended speed observer of the induction machine [19, 20] which indicates a high tolerance for parameter changes. The implemented observer structure is based on disturbance estimation as a new variable. An extended model of the five-phase induction machine was achieved by defining an additional vector in each of the *i*-th planes:

$$\zeta_{(i)} = \omega_{r(i)} \boldsymbol{\Psi}_{r(i)}. \tag{8}$$

In order to achieve the extended observer structure, the obtained components of the disturbance vectors can be added to the differential equations. The disturbances are estimated in the differential equations. The estimated errors between the measured and estimated output variables are defined by vectors as follows:

$$\tilde{\boldsymbol{i}}_{s(i)} = \boldsymbol{i}_{s(i)} - \hat{\boldsymbol{i}}_{s(i)}. \tag{9}$$

$$\tilde{\boldsymbol{\zeta}}_{(i)} = \omega_{r(i)} \hat{\boldsymbol{\psi}}_{r(i)} - \hat{\boldsymbol{\zeta}}_{(i)}, \tag{10}$$

where the superscript (^) marks the estimated variable and (~) signifies the disturbance vector. The two independent complex coordinates can be defined by two separate observers (for *i* = 1, 3). The implemented differential equations that describe the observers can be expressed as:

$$\frac{d\hat{i}_{s(i)}}{d\tau} = \left(-\frac{R_{s(i)} L_{r(i)}^2 + R_{r(i)} L_{m(i)}^2}{L_{r(i)}^2 L_{s(i)} - L_{m(i)}^2 L_{r(i)}} \right) \hat{i}_{s(i)} + \frac{R_{r(i)} L_{m(i)}}{L_{r(i)}^2 L_{s(i)} - L_{m(i)}^2 L_{r(i)}} \hat{\psi}_{r(i)} + j \frac{L_{m(i)}}{L_{r(i)} L_{s(i)} - L_{m(i)}^2} \hat{\zeta}_{(i)} + \frac{L_{r(i)}}{L_{r(i)} L_{s(i)} - L_{m(i)}^2} \boldsymbol{u}_{s(i)} +$$
$$+ k_{11(i)} \tilde{\zeta}_{(i)} + jk_{12(i)} \tilde{\zeta}_{(i)} + k_{13(i)} \tilde{\boldsymbol{i}}_{s(i)} + jk_{14(i)} \tilde{\boldsymbol{i}}_{s(i)}, \tag{11}$$

$$\frac{d\hat{\psi}_{rd(i)}}{d\tau} = \frac{R_{r(i)}}{L_{r(i)}} \hat{i}_{s(i)} + \frac{R_{r(i)} L_{m(i)}}{L_{r(i)}^2 L_{s(i)} - L_{m(i)}^2 L_{r(i)}} \hat{\psi}_{r(i)} + j\hat{\zeta}_{(i)} + k_{21(i)} \tilde{\zeta}_{(i)} + jk_{22(i)} \tilde{\zeta}_{(i)} + k_{23(i)} \tilde{\boldsymbol{i}}_{s(i)} + jk_{24(i)} \tilde{\boldsymbol{i}}_{s(i)}, \tag{12}$$

$$\frac{d\hat{\zeta}_{(i)}}{d\tau} = \frac{\Delta\hat{\omega}_{r(i)}}{\Delta t} \hat{\psi}_{r(i)} - \frac{R_{r(i)}}{L_{r(i)}} \hat{\omega}_{r(i)} \hat{i}_{s(i)} + \frac{R_{r(i)} L_{m(i)}}{L_{r(i)}} \hat{\zeta}_{(i)} + j\hat{\omega}_{r(i)} \hat{\zeta}_{(i)} + k_{31(i)} \tilde{\zeta}_{(i)} + jk_{32(i)} \tilde{\zeta}_{(i)} + k_{33(i)} \tilde{\boldsymbol{i}}_{s(i)} + jk_{34(i)} \tilde{\boldsymbol{i}}_{s(i)}, \tag{13}$$

where $k_{11} \ldots k_{34}$ are the observer gains. Finally, the angular rotor speed for each plane are calculated as follows:

$$\hat{\omega}_{r(i)} = \frac{\hat{\zeta}_{\alpha(i)} \hat{\psi}_{ra(i)} + \hat{\zeta}_{\beta(i)} \hat{\psi}_{r\beta(i)}}{\left| \hat{\psi}_{r(i)} \right|^2} .$$ (14)

2.4. Control Scheme. Figure 3 shows the dual FOC system in a closed-loop structure which are rightly associated to the fundamental and third harmonic. The decoupling and linearization lead to control of electromagnetic torque and rotor flux in separate control tracks for each i-th plane. The implemented control structure utilizes a cascades PI regulator system. The torque reference value x_1^* was obtained from the limited output of the overriding speed regulator. The synchronization unit calculates the value of x_3^* as described in section 2.2. The reference component of the stator current in the $d_{(i)}$ axis is calculated from the outer flux controller in the 1st and 3rd harmonic plane. When the reference values $i_{sd(i)}^*$, $x_{(i)}^*$ are set, the control system compares them with the actual values which are calculated from the measured and transformed stator currents. The static feedback control law is obtained as follows:

$$m_{1(i)} = x_{(i)} + \left(\frac{L_{r(i)} w_{(i)}}{R_{s(i)} L_{r(i)}^2 + R_{r(i)} L_{m(i)}^2} + \frac{L_{r(i)}}{R_{r(i)}} \right) \frac{dx_{(i)}}{d\tau},$$ (15)

$$m_{2(i)} = i_{sd(i)} + \left(\frac{L_{r(i)} w_{(i)}}{R_{s(i)} L_{r(i)}^2 + R_{r(i)} L_{m(i)}^2} \right) \frac{di_{sd(i)}}{d\tau}.$$ (16)

Finally, based on the decoupling and outputs of the torque and current controllers, $m_{1(i)}$, $m_{2(i)}$, stator voltage components in $d_{(i)} - q_{(i)}$ axes are calculated as follows:
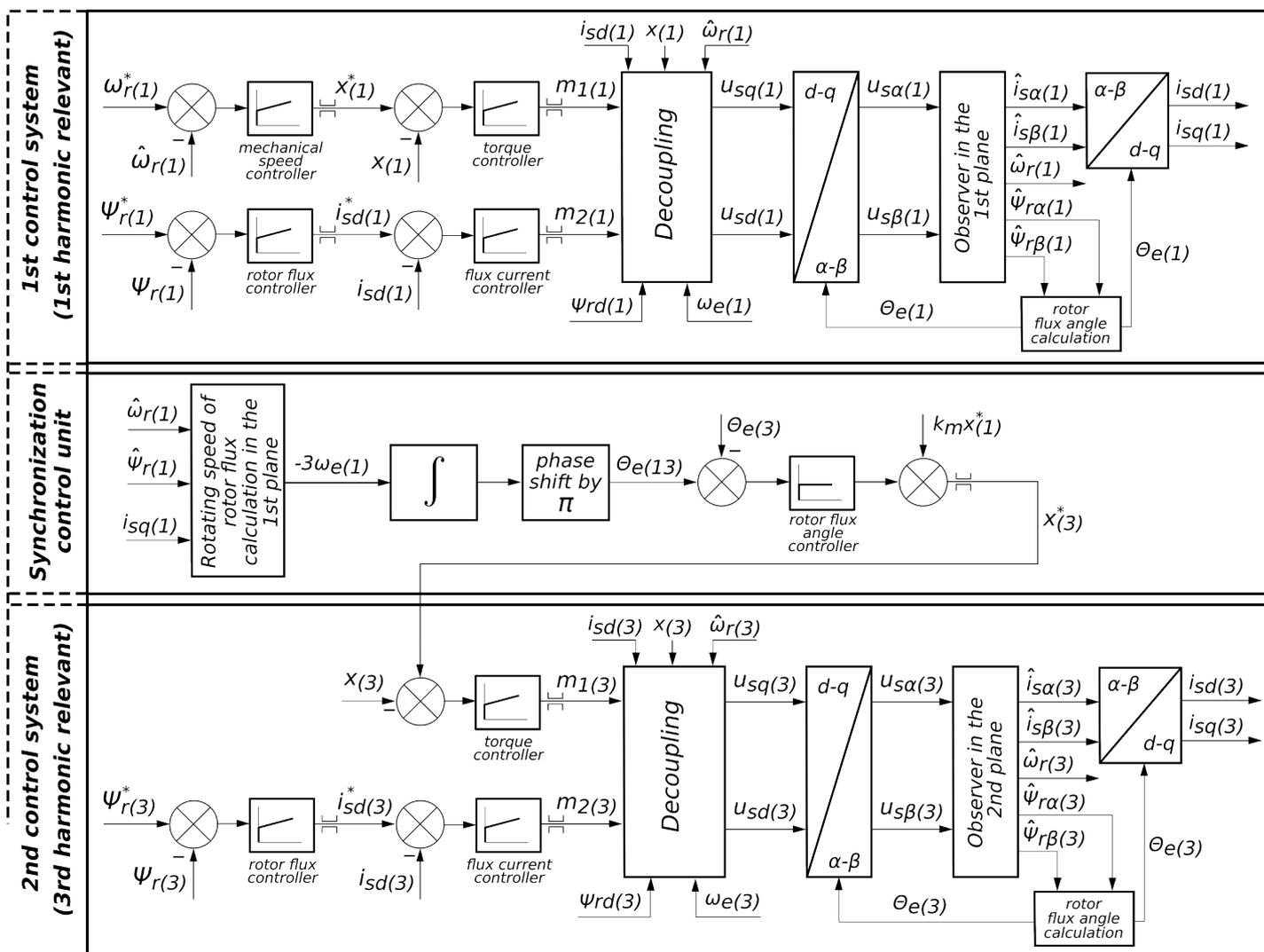

Fig. 3. The implemented FOC scheme in dual vector plane: the 1st control system is related to the control of the fundamental harmonic rotor flux and the 2nd control system is related to the control of the 3rd harmonic rotor flux

www.czasopisma.pan.pl   PAN   www.journals.pan.pl

Sensorless field oriented control for five-phase induction motors with third harmonic injection and fault insensitive feature

$$u_{sd(i)} = \left(\frac{L_{r(i)}L_{s(i)} - L_{m(i)}}{L_{r(i)}}\right)\left(\frac{R_{s(i)}L_{r(i)}^2 + R_{r(i)}L_{m(i)}^2}{L_{r(i)}^2 L_{s(i)} - L_{m(i)}^2 L_{r(i)}}\right)m_{2(i)} - \left(\frac{L_{r(i)}L_{s(i)} - L_{m(i)}}{L_{r(i)}}\right)\left(\omega_{e(i)}\frac{x_{(i)}}{\psi_{rd(i)}} - \left(\frac{R_{r(i)}L_{m(i)}}{L_{r(i)}^2 L_{s(i)} - L_{m(i)}^2 L_{r(i)}}\right)\psi_{rd(i)}\right), \qquad (17)$$

$$u_{sq(i)} = \left(\frac{L_{r(i)}L_{s(i)} - L_{m(i)}}{L_{r(i)}}\right)\left(\frac{R_{s(i)}L_{r(i)}^2 + R_{r(i)}^2 L_{m(i)}^2}{L_{r(i)}^2 L_{s(i)} - L_{m(i)}^2 L_{r(i)}} + \frac{R_{r(i)}}{L_{r(i)}}\right)\left(m_{1(i)} + \omega_{e(i)}i_{sd(i)}\psi_{rd(i)} + \frac{L_{m(i)}\omega_{r(i)}\psi_{rd(i)}^2}{L_{r(i)}L_{s(i)} - L_{m(i)}} - \frac{R_{r(i)}L_{m(i)}}{L_{r(i)}}\frac{i_{sd(i)}x_{(i)}}{\psi_{rd(i)}}\right). \qquad (18)$$
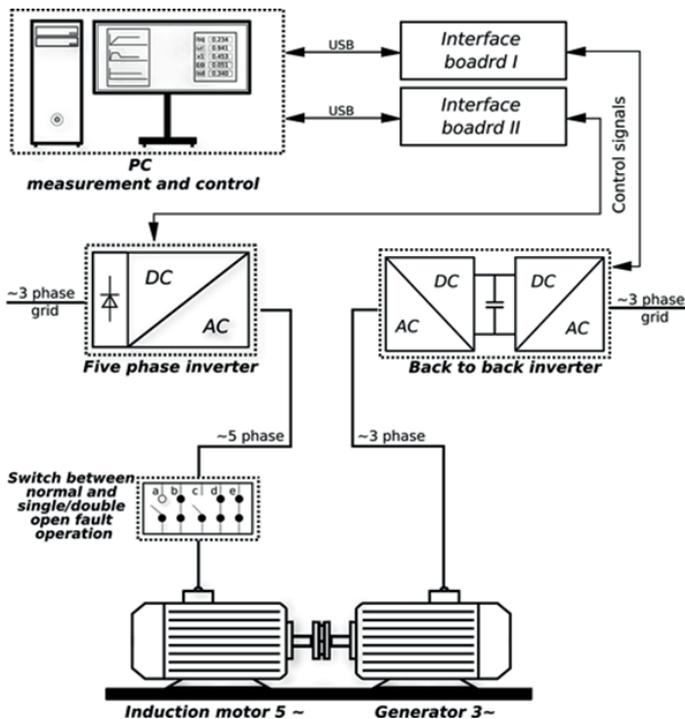

Fig. 4. The structure of the test bench

3. Test bench

The investigation of the proposed control system in the both planes was performed with a 5.5 kW, two pole, five-phase induction motor. The control algorithm structure was implemented to the Digital Signal Processor SHARC ADSP-21363 as shown in Fig. 3. The PWM vector method based on six active vectors, proposed in [23, 24] was utilized in order to generate reference stator voltage, calculated as the control system output. The measured variables are the five stator currents which are transformed to four components: $i_{s\alpha1}$, $i_{s\beta1}$, $i_{s\alpha3}$, $i_{s\beta3}$. These variables as well as the generated stator voltage vector components, i.e. $u_{s\alpha1}$, $u_{s\beta1}$, $u_{s\alpha3}$, $u_{s\beta3}$, being the known values, are brought to the observer block. Figure 4 presents the overall structure of the implemented test setup. In order to investigate the drive system in healthy and faulty conditions under load, a five-phase induction machine was coupled with a three phase generator. The generator was supplied by a back to back inverter to ensure maximum load ability. The generator control system is based on multiscalar variables and allows for accurate load torque changes as described in [25]. Moreover, the test bench

is equipped with a high precision torque sensor (ETH DRFL), which was used in mechanical characteristics preparation, as shown in Fig. 14.

4. Experimental investigations

4.1. Healthy drive condition. The initial tests were carried out for two dynamic modes, i.e. machine speed increase and reverse, under load for healthy drive conditions. First, the dual FOC system with synchronized 3rd harmonic injection was investigated. The variable limit correlated to the generated electromagnetic torque x_1 in the first vector plane was set to 1.0 p.u. To reduce the peak rotor flux to the rated value, the reference level of Ψ_{rd1} was increased to 1.1 p.u. and the amplitude of injected third harmonic rotor flux was set to 0.15 p.u. This way, by injecting the third harmonic, the summary flux reaches its top equal to 0.95 p.u., which enabled an unsaturated operation in the magnetic circuit of the induction motor. Figure 5 presents
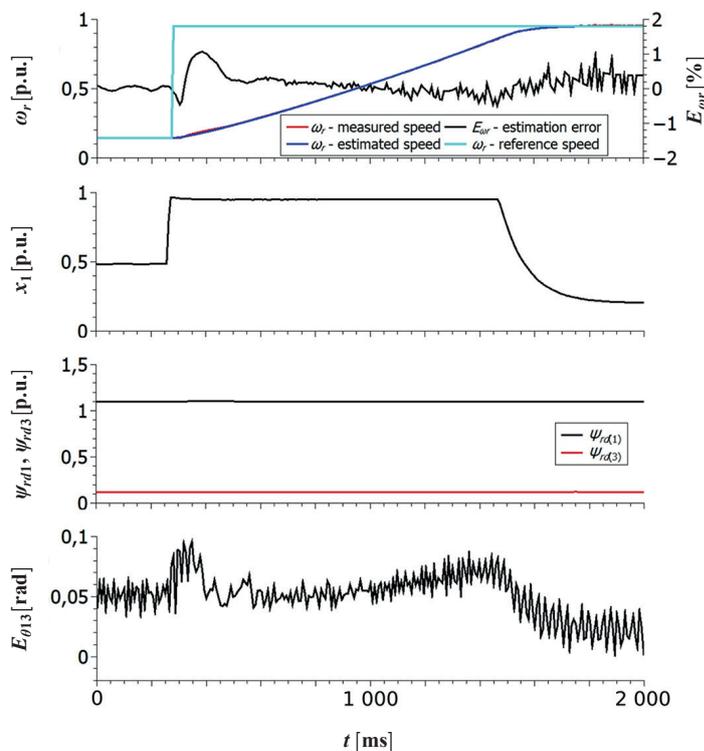

Fig. 5. Motor speed increase from $\omega_r = 0.15$ p.u. to $\omega_r = 0.95$ p.u. with third harmonic injection under load ($T_L \approx 0.5$ p.u.)

the characteristic controlled values during the step change of the required rotor speed command from 0.15 p.u. to 0.95 p.u. with 3rd harmonic injection. The reference value corresponding to the torque x_3 in the second plane was limited to 0.15 p.u. The dynamic of the flux synchronization loop is reflected by the error position between two vectors.

Figure 6 presents the machine reverse from $\omega_r = 0.6$ p.u. to $\omega_r = -0.6$ p.u. with a vector control in both planes. Figure 5 and Fig. 6 shows that the synchronization loop assures the same relative angular speeds of each harmonic rotor flux, which is reflected by the field position error $E_{\theta e13}$ which is close to zero. The flux vector modules $\Psi_{rd(i)}$ were maintained at their reference values during dynamic operation and speed reversing. Figure 8 presents a comparison of the observer rotor speed increase, from $\omega_r = 0.2$ p.u. to 0.75 p.u., using conventional and
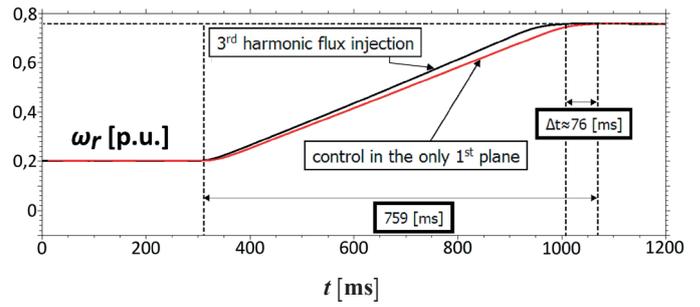

Fig. 8. Motor speed increase comparison from $\omega_r = 0.2$ p.u. to 0.75 p.u., using conventional and dual plane FOC

dual plane FOC. The quasi-trapezoidal rotor flux waveform (see Fig. 7) decreased the rotor speed rise time by approximately 10% and confirmed the presumption of the output motor torque increase.

4.2. Single-phase open fault. To prove the performance of the control system under open phase fault, experimental tests were carried out at dynamic modes with four phases: the speed increase and the reverse under load condition. Figure 9 presents the specific controlled values in the first plane only during the step change of the desired rotor speed command from 0.15 p.u. to 0.95 p.u. under load $T_L \approx 0.5$ p.u. Oscillations of electromagnetic torque related to postfault condition and reduction of switching states number are clearly visible. However, the drive is capable to hold the required speed and flux in the system.
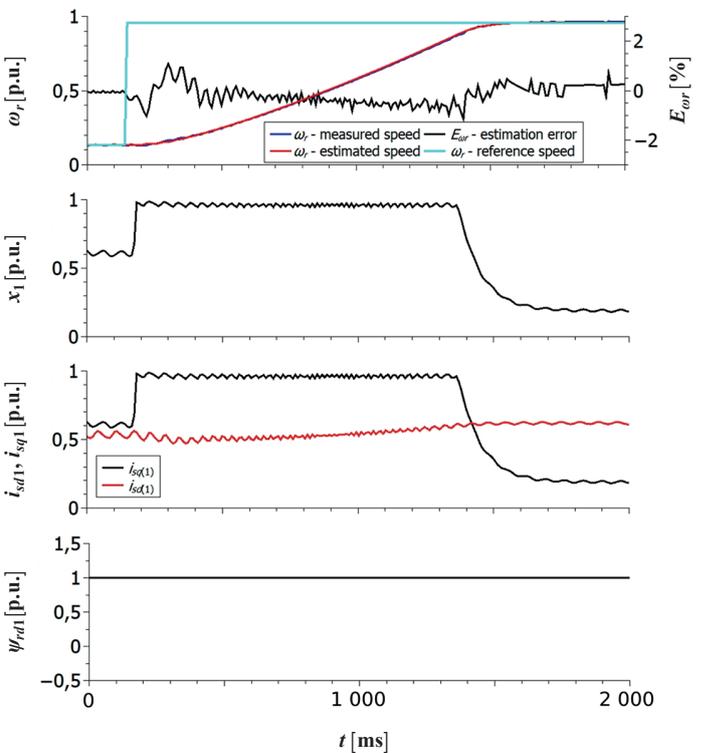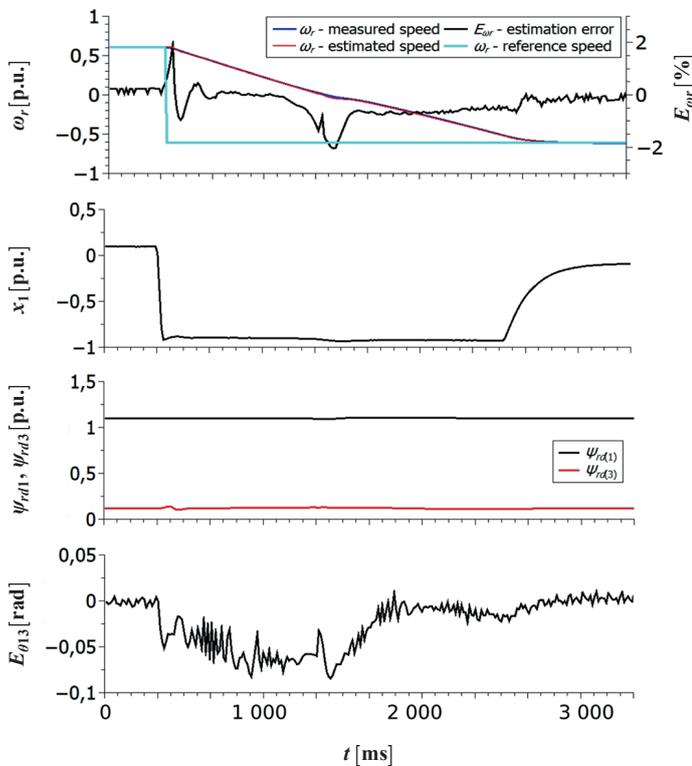

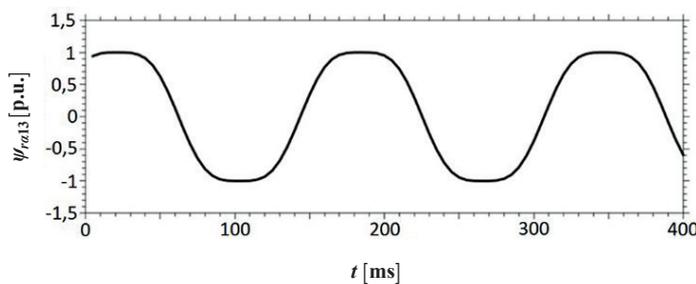Fig. 6. Machine reverse from $\omega_r = 0.6$ p.u. to $\omega_r = -0.6$ p.u. with the third harmonic injection

Fig. 7. Resulting flux waveform in α axis in steady mode:
$$\psi_{r\alpha13} = \psi_{r\alpha1} + \psi_{r\alpha3}$$

Fig. 9. Rotor speed increase from $\omega_r = 0.15$ p.u. to $\omega_r = 0.95$ p.u. under open phase fault ($T_L \approx 0.5$ p.u.)

www.czasopisma.pan.pl   PAN   www.journals.pan.pl

Sensorless field oriented control for five-phase induction motors with third harmonic injection and fault insensitive feature

Figure 10 presents the machine reverse from $\omega_r = -0.7$ p.u. to $\omega_r = 0.7$ p.u. The critical part is the close to zero speed region. Nevertheless the control system is able to handle the speed reverse on four phases. The experimental results prove the implemented control system is able to handle the postfault condition with one open phase in a speed increase and reverse operation. The flux vector module Ψ_{rd} is maintained at the reference value during dynamic operation, even in the speed reversing. Motor torque ripple occurred when the rotor speed was near to zero. This is the consequence of the rotor flux vector estimation error for low speed area operation and analyzed fault condition.
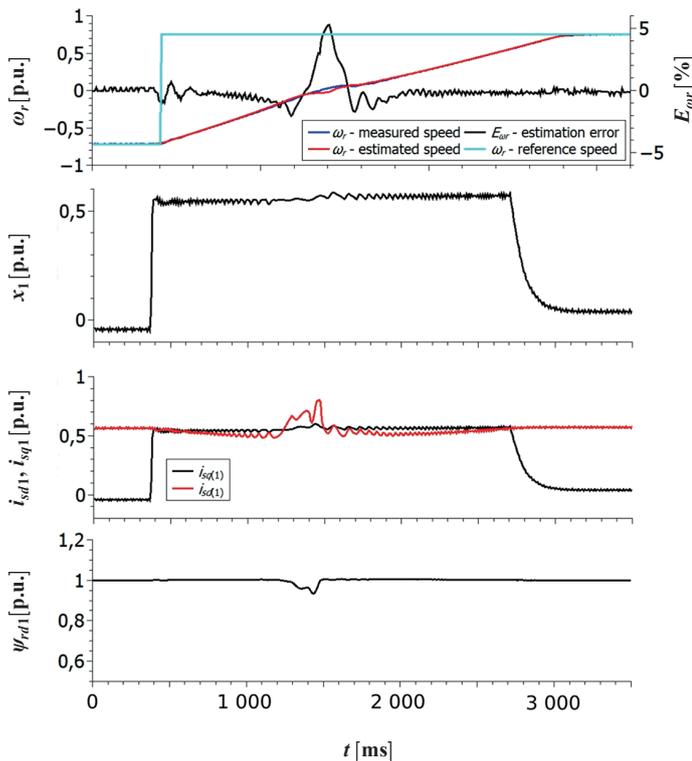

Fig. 10. Motor speed reverse from $\omega_r = -0.7$ to $\omega_r = 0.7$ under single-phase fault

4.3. Double-phase open fault. The next experiment presents the operation of the drive system with two open phases. Figure 11 shows a rotor speed increase from $\omega_r = 0.2$ p.u. to $\omega_r = 0.95$ p.u. under load ($T_L \approx 0.5$ p.u.), where Fig. 12 presents the machine reverse from $\omega_r = 0.7$ p.u. to $\omega_r = -0.8$ p.u. As can be seen in Fig. 11 and Fig. 12 the drive system is able to operate evenly two open phases. The observer structure is able to handle this notorious change of parameter without any correction of the observer coefficients which proofs its usability for a fault tolerant control. As can be seen in Fig. 10 and Fig. 12, rotor speed estimation error is increasing significantly, when rotor speed is near to zero. This is the consequence of the rotor flux estimation error for low speed area operation and primarily reason for failure occurrence. Nevertheless, the rotor speed observer remained stable, which confirms its insensitivity to fault conditions.
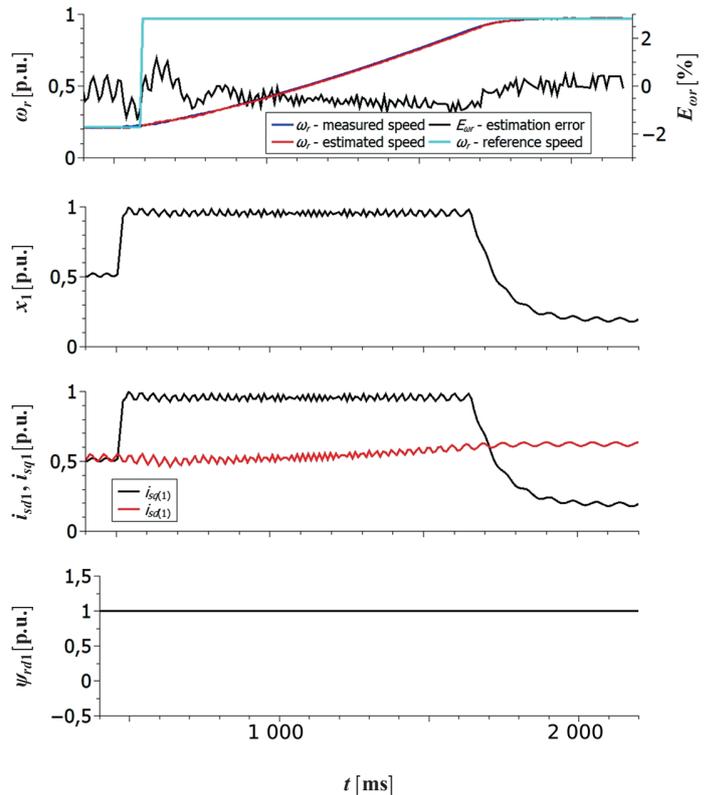

Fig. 11. Rotor speed increase from $\omega_r = 0.2$ to $\omega_r = 0.95$ under double-phase fault ($T_L \approx 0.5$ p.u.)
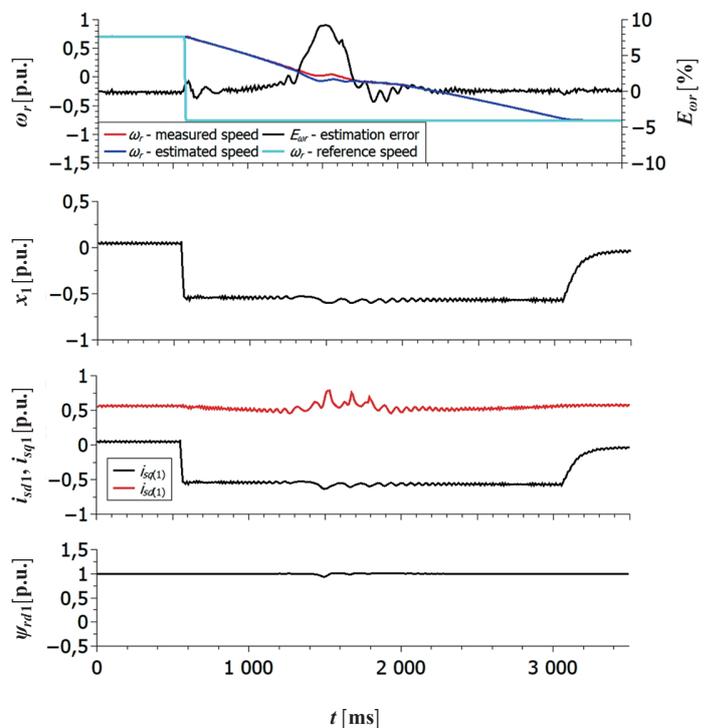

Fig. 12. Motor speed reverse from $\omega_r = 0.7$ to $\omega_r = -0.8$ under double-phase fault

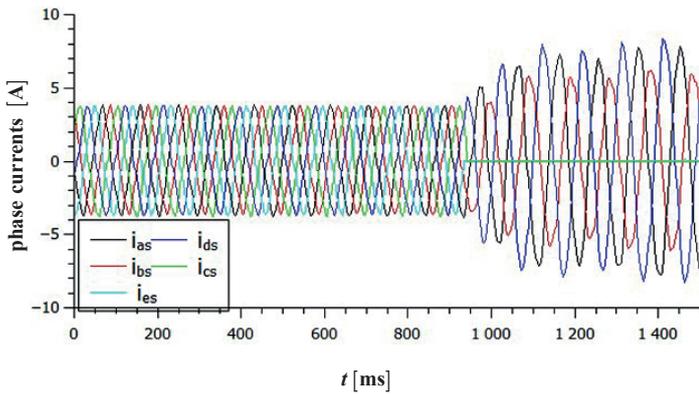F. Wilczyński, P. Strankowski, J. Guziński, M. Morawiec, and A. Lewicki

Fig. 13. Phase currents under double-phase fault

Obtaining the electromagnetic torque under double-phase open is associated with stator currents values increase in healthy phases. The difference between phase stator currents values in normal and faulty situation is presented in Fig. 13.

4.4. Open phase fault operation. To prove reliability of the proposed five-phase induction motor control system different experimental tests have been performed under post-fault situation. The essential control criterion in faulty operation is to minimize modifications which must be introduced when open-phase occurs. In the proposed control system changes related with the number of freedom degrees reduction [16, 17] and pulse width modulation (PWM) are not considered. Hence, in order to identify the possibilities of a faulted five-phase induction motor Fig. 14 presents speed-torque and current-torque characteristics of the Finite Elements Method simulation for

five-phase motor V/f = const control system and the real drive under load in healthy and under fault conditions. Figure 14 shows that the current is rising compare to the healthy state if a phase is open in the system. Nevertheless the motor is able to produce torque. It is also thinkable to increase the current in the other phases in order to obtain the nominal torque. If two open phase faults occurs the motor is able to provide torque only if opposite phases are open. It two consecutive phases are open the motor torque is disappear so the drive will not work, as can be seen in Fig. 14. However, in order to operate the induction motor under fault and even if the observer is capable to handle the parameter changes it is recommended to optimize the control structure to prevent a total drive failure. When open phase fault appears, modifications in the control system include only regulator gains and output limit. Moreover, control system related with 3rd harmonic is switching off because of the voltage vectors number decreasing and impossibility of third harmonic generation. Properties of used speed observer structure allow to estimate the induction machine state variables even under double-phase fault. Insensitivity of the speed observer complete with the linearized FOC control constitute a sensorless, more reliable and flexible drive system.

The authors designed a postfault condition algorithm that was applied to the control to ensure a reliable operation of the drive system. The structure of the algorithm is shown in Fig. 15. The samples of phase current are written into a ring buffer. After the current sampling a zero detection of the values is applied which results of each phase to be counted. If one open phase is detected the 3rd harmonic will be turned, the control parameter will be changed to a smoother control to avoid current peaks and a drive warning will be displayed for the operator. In case of two open phases the algorithm detects which of two phases are
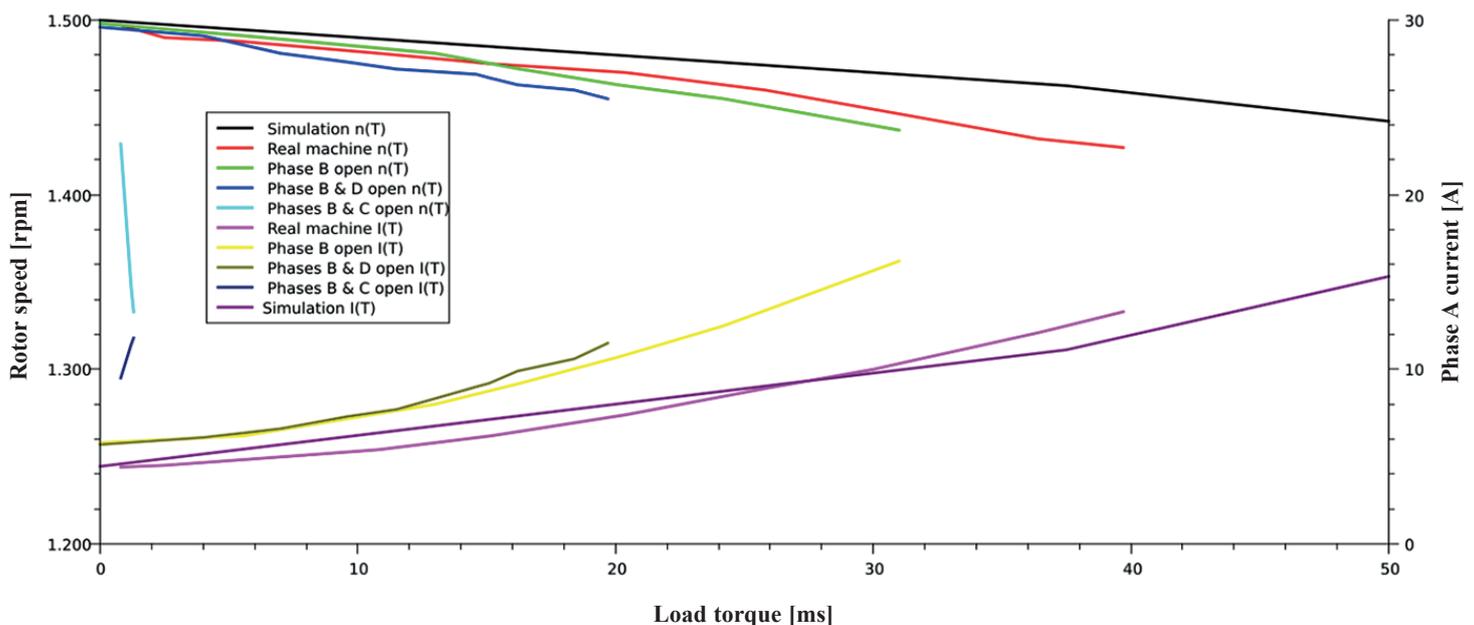

Fig. 14. Speed-torque $n(T)$ and current-torque $I(T)$ characteristics for healthy and fault motor operations for V/f = const control
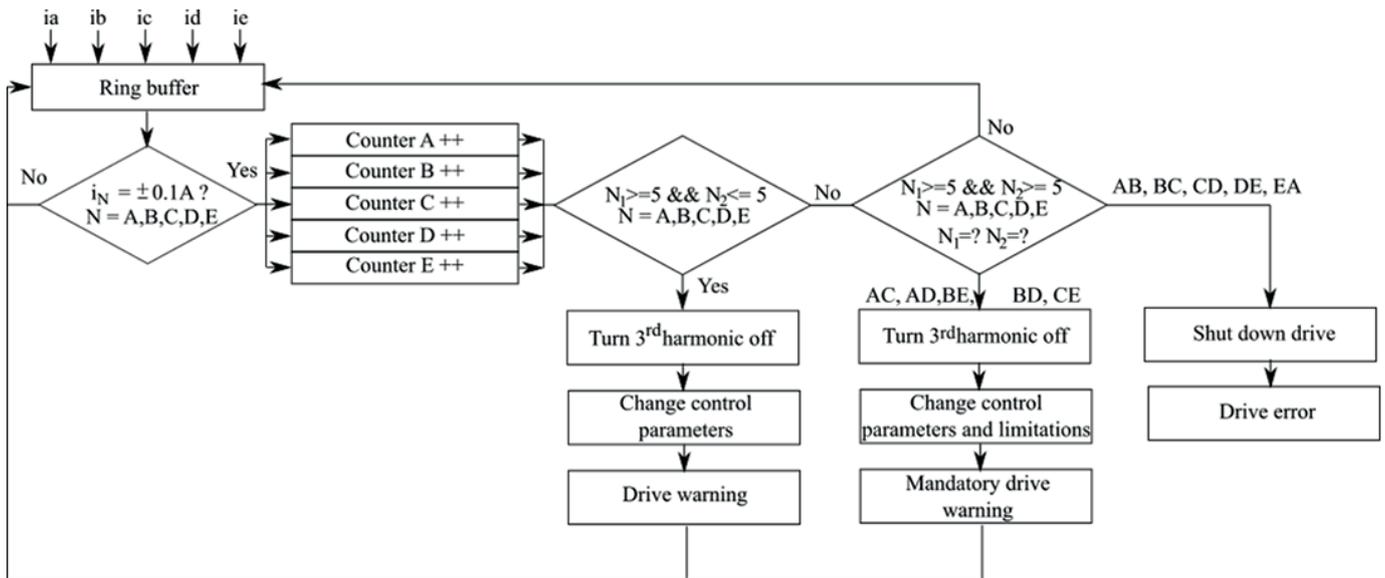
260

www.czasopisma.pan.pl   PAN   www.journals.pan.pl

Sensorless field oriented control for five-phase induction motors with third harmonic injection and fault insensitive feature

Fig. 15. Motor fault detection algorithm

open. If two opposite phases are open the system will turn off the 3rd harmonic, change the control parameters to less dynamic control. The control limits will be set lower in order to avoid motor damage and a critical warning will be displayed for the operator. If two neighbor phases are open the system is incapable to run and will be shut off in order to prevent any drive damages. All values for the algorithm are chosen empirically from the experiment and proof to be reliable.

5. Conclusion

The paper presents an implementation of a five-phase vector control system that includes two independent control structures. One structure is responsible for generating the fundamental harmonic and the other structure is responsible for the third stator voltage harmonic. The proposed machine model linearization enables the control of decoupled torque and rotor flux values in two independent planes. It is empirically confirmed that the described five-phase IM control system with the 3rd harmonic injection allows to increase the torque value by approximately 10%. Furthermore, the paper presents an implementation of a precise and parameter change insensitive speed observer which enabled a reliable sensorless control. Even if the two independent planes require a higher computational effort the presented FOC implementation with 3rd harmonic injection enriches the possibilities for an further implementation for an industry drive system. The torque enhancement in connection with the increased reliability of the five-phase system offers new perspectives on the field of automation systems, drive systems for electrical vehicles, aircraft actuators as well as traction drives. Moreover, the implemented control structure acquires fault tolerant properties and allows for possible running with limited operation capabilities even under double-phase fault.

The postfault performance of the analyzed drive with mechanical characteristics is presented.

References

[1] E.E. Ward and H. Härer, "Preliminary investigation of an inverter-fed 5-phase induction motor", *PROC. IEE*, vol. 116, No. 6, 1969.

[2] C.C. Scharlau, L.F.A. Pereira, and L.A. Pereira, "Performance of a five-phase induction machine with optimized air gap field under open loop V/f control", *IEEE Transaction*, vol. 23, no. 4, 2008.

[3] O. Ellabban and H. Abu-Rub, "Field Oriented Control of a Five Phase Induction Motor Fed by a Z-Source Inverter", *IEEE International Conference on Industrial Technology* (ICIT), pp. 1624–1629, 2013.

[4] H. Xu, H.A. Toliyat, and L.J. Petersen, "Five-Phase Induction Motor Drives with DSP-Based Control System", *IEEE International Electric Machines and Drives Conference* (Cat. No. 01EX485), pp. 304–309, 2001.

[5] M.A. Elgenedy, A.S. Abdel-Khalik, A.M. Massoud, and A. Ahmed, "Indirect Field Oriented Control of Five-Phase Induction Motor Based on SPWM-CSI", *International Conference on Electrical Machines* (ICEM), pp. 2101–2106, 2014.

[6] L. Zheng, J.E. Fletcher, B.W. Williams, and X. He, "Dual-Plane Vector Control of Five-Phase Induction Machine for Improved Flux Pattern", *IEEE Transactions*, vol. 55, no. 5, pp. 1996–2005, 2008.

[7] K. Min-Huei, K. Nam-Hun, and B. Won-Sik, "A Five-Phase IM Vector Control System Including 3rd Current Harmonics Component", *8th International Conference on Power Electronics – ECCE Asia*, pp. 2519–2524, 2011.

[8] J.A. Riveros, J. Prieto, F. Barrero, S. Toral, M. Jones, and E. Levi, "Predictive Torque Control for five-phase induction motor drives", *IECON 2010 – 36th Annual Conference on IEEE Industrial Electronics Society*, pp. 2467–2472, 2010.

[9] H.A. Toliyat and X. Huangsheng, "A novel direct torque control (DTC) method for five-phase induction machine", *APEC 2000, Fifteenth Annual IEEE Applied Power Electronics Conference and Exposition*, vol. 1, pp. 162–168, 2000.

[10] M. Adamowicz, J. Guziński, and Z. Krzemiński, "Nonlinear Control of Five Phase Induction Motor with Synchronized Third Harmonic Flux Injection", (SGRE), 2015.

[11] E. Levi, R. Bojoi, F. Profumo, H.A. Toliyat, and S. Williamson, "Multiphase induction motor drives – a technology status review, in Electric Power Applications", *IET*, vol. 1, no. 4, 489–516, 2007.

[12] S. Williamson and S. Smith, "Pulsating torque and losses in multiphase induction machines, in Industry Applications", *IEEE Transactions*, vol. 39, no. 4, 986–993, 2003.

[13] A.S. Abdel-Khalik, M.I. Masoud, and B.W. Williams, "Improved Flux Pattern With Third Harmonic Injection for Multiphase Induction Machines", *IEEE Transactions on Power Electronics*, vol. 27, no. 3, 1563–1578, 2012.

[14] A.S. Abdel-Khalik, S.M. Gadoue, M.I. Masoud, and B.W. Wiliams, "Optimum Flux Distribution With Harmonic Injection for a Multiphase Induction Machine Using Genetic Algorithms", *IEEE Transactions on Energy Conversion*, vol. 26, no. 2, 501–512, 2011.

[15] H.A. Toliyat, T.A. Lipo, and J.C. White "Analysis of a concentrated winding induction machine for adjustable speed drive applications – Part 1: Motor Analysis", *IEEE Trans. Energy Convers.*, vol. 6, no. 4, 679–683, 1991.

[16] H. Guzman, M.J. Duran, F. Barrero, B. Bogado, and S. Toral, "Speed Control of Five-Phase Induction Motors With Integrated Open-Phase Fault Operation Using Model-Based Predictive Current Control Techniques", IEEE Transactions, vol. 61, no. 9, 4474–4484, 2014.

[17] M. Bermudez, I. Gonzalez-Prieto, F. Barrero, H. Guzman, M.J. Duran, and X. Kestelyn, "Open-Phase Fault-Tolerant Direct Torque Control Technique for Five-Phase Induction Motor Drives", *IEEE Transactions*, vol. 64, no. 2, 902–911, 2014.

[18] H.A. Toliyat, T.A. Lipo, and J.C. White, "Analysis of a concentrated winding induction machine for adjustable speed drive applications – Part II: Motor design and performance", *IEEE Trans. Energy Convers.*, vol. 6, no. 4, pp. 684–692, 1991.

[19] M. Morawiec, P. Strankowski, A. Lewicki, and J. Guzinski, "Sensorless control of five-phase induction machine supplied by the VSI with output filter", *10th International Conference on Compatibility*, *Power Electronics and Power Engineering*, pp. 304–309, 2016.

[20] Z. Krzemiński, A. Lewicki, and M. Morawiec, "Speed observer based on extended model of induction machine", *IEEE International Symposium on Industrial Electronics* (ISIE), 2010.

[21] Z. Krzeminski, "Observer of induction motor speed based on exact disturbance model", Int. Conf. EPE-PEMC'2008, Poznan, Poland, 2008.

[22] M. Morawiec and J. Guzinski, "Sensorless control system of induction machine supplied by voltage source inverter with output filter", 17th EPE'15 ECCE-Europe, 2015.

[23] A. Lewicki, J. Guziński, and P. Strankowski, "Space-Vector Modulation for five-phase Voltage Source Inverter", XII Conf. SENE 2015, 18–20, 2015.

[24] A. Lewicki, J. Guziński, and P. Strankowski, "Five-Phase Voltage Source Inverter Space-Vector Modulation Method", *Electrical Review* R.92 NR 4/2016.

[25] P. Strankowski, J. Guziński, M. Morawiec, A. Lewicki, and F. Wilczyński, "Sensorless disturbance detection for five phase induction motor with third harmonic injection", *11th IEEE International Conference on Compatibility*, *Power Electronics and Power Engineering* (CPE-POWERENG), Cadiz, 2017, pp. 387–391.